

Object-centric Video Question Answering with Visual Grounding and Referring

Haochen Wang^{1*}, Qirui Chen^{2*}, Cilin Yan³, Jiayin Cai³,
Xiaolong Jiang³, Yao Hu³, Weidi Xie^{2†}, Stratis Gavves¹

¹University of Amsterdam ²SAI, Shanghai Jiao Tong University ³Xiaohongshu Inc.

Abstract

Video Large Language Models (VideoLLMs) have recently demonstrated remarkable progress in general video understanding. However, existing models primarily focus on high-level comprehension and are limited to text-only responses, restricting the flexibility for object-centric, multi-round interactions. In this paper, we make three contributions: (i) we address these limitations by introducing a VideoLLM model, capable of performing both object referring for input and grounding for output in video using both textual and visual prompts; (ii) we propose **STOM** (Spatial-Temporal Overlay Module), a novel approach that propagates arbitrary visual prompts input at any single timestamp to the remaining frames within a video; (iii) we present **VideoInfer**, a manually curated object-centric video instruction dataset featuring question-answering pairs that require reasoning. We conduct comprehensive experiments on VideoInfer and other existing benchmarks across video question answering and referring object segmentation. The results on 12 benchmarks of 6 tasks show that our proposed model consistently outperforms baselines in both video question answering and segmentation, underscoring its robustness in multimodal, object-centric video and image understanding. Project page: <https://qirui-chen.github.io/RGA3-release/>.

1. Introduction

Video question answering (VideoQA) refers to the task that enables machines to understand and reason about videos. As a natural way for both humans and embodied agents (e.g., robots or virtual assistants) to perceive the world, videos capture rich, continuous streams of data with complex spatial-temporal information, such as dynamic scenes, evolving interactions, and object behaviors. Despite the tremendous progress, existing Video Large Lan-

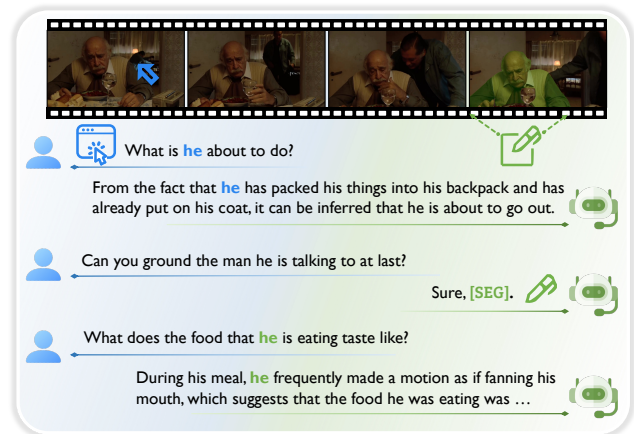


Figure 1. **RGA3** enables both **referring** and **grounding** capabilities for object-centric video understanding. In contrast to previous VideoLLMs, which are limited to text-only responses with mask reference, RGA3 can process arbitrary **visual prompts** and generate both textual answers and **segmentation masks**.

guage Models (VideoLLMs) [9, 13, 14, 30, 33, 61, 71] have primarily focused on holistic scene comprehension, such as answering high-level questions about videos, rather than addressing fine-grained spatial-temporal queries on objects, limiting their ability to resolve detailed object-centric reasoning in complex, dynamic video content.

This paper proposes to advance the task of multimodal, object-centric video understanding by introducing **RGA3** (**R**efer and **G**round **A**nanything **A**nytime at **A**ny Granularity), a unified framework designed to ground objects of interest and answer detailed questions about them in videos. In detail, the resulting model enables: (i) integrating arbitrary visual prompts—such as masks, bounding boxes, arrows, points, or scribbles—with textual inputs to perform complex reasoning tasks about specific objects in videos, and (ii) processing video and textual queries to generate segmentation masks for objects referred to in the query. By combining these capabilities, RGA3 facilitates object-centric reasoning, enabling more precise and interactive video understanding.

*Both authors contribute equally to this work.

†Corresponding author.

Our core innovation of **RGA3** lies in two components that enable object-centric video reasoning. The first is the Spatial-Temporal Overlay Module (STOM), which allows the model to process arbitrary visual prompts—such as masks, bounding boxes, arrows, points, or scribbles—at any timestamp within a video. This enhances the model’s interactivity and flexibility in handling spatial-temporal reasoning tasks. The second is to unify the object-centric question-answering and segmentation tasks for both images and videos based on the multimodal large language models (MLLMs) and SAM2 [49], which enables the generation of segmentation masks for the referred objects in the query, while simultaneously reasoning over visually grounded questions. By integrating these two designs, **RGA3** provides a unified framework for fine-grained object grounding and reasoning in videos.

In addition to the development of model architecture, we introduce an object-centric video instruction dataset with manually crafted questions and reasoning process in the answers, namely **VideoInfer**. Unlike existing datasets [69], which construct questions through automated pipelines that largely focus on object descriptions, resulting in a large proportion of perception questions, our proposed dataset emphasizes reasoning and long-term temporal understanding. VideoInfer contains around 29K question-answer (QA) pairs, and significantly surpasses existing datasets in question complexity and reasoning depth. We conduct extensive evaluations of RGA3 on VideoInfer as well as 11 existing benchmarks, including referring visual question-answering and referring/reasoning object segmentation tasks at both image and video levels. The results demonstrate that RGA3 achieves state-of-the-art performance across both referring and grounding tasks.

The rest of the paper is organized as follows: In Sec. 2, we provide an overview of recent Multi-modal Large Language Models (MLLMs) and existing approaches for referring and grounding tasks; Sec. 3 details our proposed RGA3 framework and the VideoInfer dataset collection process; Sec. 4 presents the implementation details and reports extensive experimental results and analysis on VideoInfer as well as 11 existing benchmarks.

2. Related Work

Multimodal Large Language Models (MLLMs). Recent research in multimodal models has focused on visual instruction tuning, where pre-trained LLMs are fine-tuned for image and video understanding tasks. Models such as LLaVA [36], MiniGPT-4 [76], mPLUG-Owl [64], Otter [27], and InstructBLIP [36] have demonstrated significant progress by aligning vision-language representations through instruction tuning. Beyond text generation, recent works such as [24, 25, 37, 52] have further extended the capabilities of MLLMs to retrieval and generation tasks,

showcasing the growing versatility of MLLMs.

Video Large Language Models (VideoLLMs). Extending image-level MLLMs to the video domain presents unique challenges, since videos comprise dynamic sequences that encode temporal dependencies, requiring models to process both spatial and temporal information. Models such as Video-LLaVA [33], Video-ChatGPT [61], and Intern-Video [57, 58] have shown strong performance in tasks like video captioning, temporal reasoning, and commonsense understanding, enabling text-based interaction with video content. Despite these advancements, existing VideoLLMs largely focus on holistic scene understanding, generating high-level textual descriptions of videos, while failing to capture fine-grained object interactions or nuanced temporal dependencies [28, 29, 74]. This limitation restricts their ability for object-centric reasoning, which is critical for detailed video analysis and practical real-world applications.

Object-centric MLLMs. In the recent literature, the tasks of object-centric referring and grounding have been well-studied in the image domain, with models like GPT4ROI [73], Ferret [65], and Osprey [68] for fine-grained object understanding via region-based visual prompts. Extending these capabilities to videos is more challenging due to their temporal complexity. Recent works, such as VISA [60], VideoLISA [4], and some concurrent works like VideoRefer [69], GLUS [35], DAM [32], and Sa2VA [67], focus on either only mask-based referring question-answering or object grounding. In contrast, we aim to develop a unified framework for both tasks, which does not require accurate object reference (*i.e.*, masks) and supports arbitrary visual prompts (*e.g.*, boxes, points, or scribbles) at any timestamp, enabling precise, multi-round, object-centric reasoning in videos.

3. Method

In this section, we will present details on the RGA3 architecture and the dataset collection procedure for VideoInfer as follows: Sec. 3.1 introduces the considered problem; Sec. 3.2 details the model architecture; Sec. 3.3 describes the dataset collection process of VideoInfer, along with statistical analysis; Sec. 3.4 describes the instruction tuning process, in which we finetune RGA3 on VideoInfer and existing datasets through a co-training strategy.

3.1. Problem Formulation

Given a video of frame sequences, our goal in this paper is to build a model $\phi_\theta(\cdot)$ to answer questions \mathcal{Q} given an (optional) visual prompt P_t at frame t :

$$\mathcal{A}, \mathcal{M} = \phi_\theta(\mathcal{V}, \mathcal{Q}, P_t),$$

where $\mathcal{V} \in \mathbb{R}^{T \times H \times W \times 3}$ is the input video containing T frames, $P_t \in \mathbb{R}^{H \times W \times 4}$ is arbitrary visual prompt (bound-

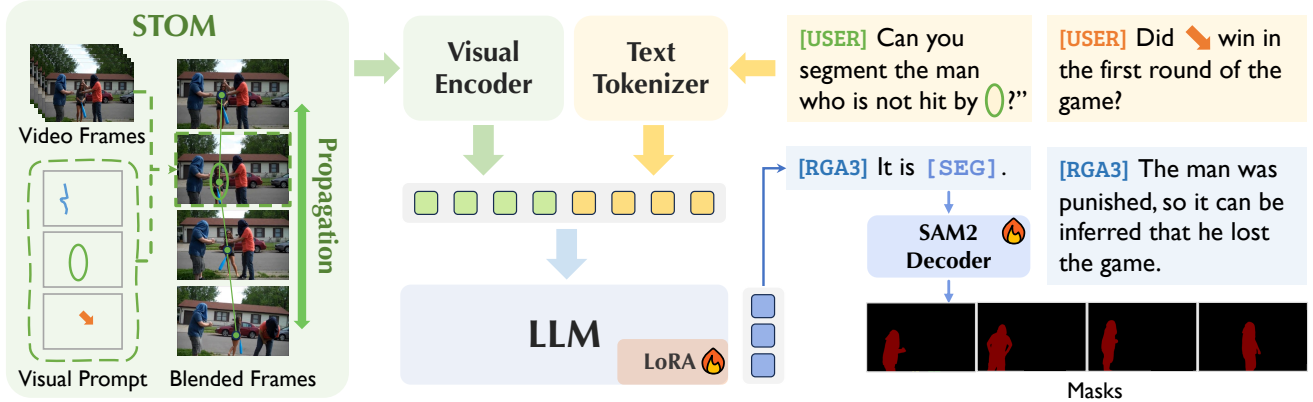


Figure 2. **The proposed RGA3 architecture overview.** (a) The Spatial-Temporal Overlay Module (STOM) is introduced to process arbitrary visual prompts (e.g., scribble, ellipse, arrow, etc.) at any timestamp and propagate to all frames, allowing for interactive object-centric reasoning and continual visual attention. (b) A visual encoder is employed to extract video representations of overlaid frames processed through STOM. (c) A Large Language Model (LLM) takes the concatenated sequence of visual and text tokens as input and generates responses. (d) To facilitate reasoning-based video object segmentation, a SAM2 decoder is incorporated for generating segmentation masks when prompted with a [SEG] token, extending RGA3’s capabilities beyond text-only responses.

ing boxes, masks, scribbles, arrows, or points) represented by a RGBA mark with color and alpha channels. Q and A are questions and answers in text. $\mathcal{M} \in \mathbb{R}^{T \times H \times W}$ denotes the generated (optional) segmentation masks when users refer to objects in the answer. Consequently, the model is able to process both textual input and visual prompts, jointly reasoning over spatial-temporal relationships to generate an output response, consisting of textual answers and segmentation masks to highlight the referred objects in the video, as demonstrated in Fig. 1.

3.2. RGA3 Architecture

The overall architecture of our proposed RGA3 is illustrated in Fig. 2. RGA3 employs a visual encoder to compute global video representations and a pretrained text tokenizer to get language embeddings. To facilitate region-based referring, we propose STOM, a Spatial-Temporal Overlay Module that propagates arbitrary visual prompts input at any timestamp to the remaining frames for long-term video object referring. Additionally, we incorporate the SAM2 [49] decoder to generate segmentation masks, extending RGA3’s capabilities beyond text-only responses.

Visual Prompting. A visual prompt P_t , e.g., masks, boxes, or scribbles at timestamp t is represented as an RGBA image $P_t \in \mathbb{R}^{H \times W \times 4}$, where the mark is colored, and the background is opaque. STOM propagates visual prompt P_t at frame t to all frames $\{P_1, P_2, \dots, P_T\}$ to get comprehensive object referring. Specifically, we adopt an off-the-shelf point tracker [20] to track points around the centroid of the visual prompt bi-directionally. The pixels to be tracked are defined as $\{\mathbf{p} \in \mathbb{R}^2 \mid |\mathbf{p} - \mathbf{c}|_2 \leq r\}$, where $\mathbf{c} \in \mathbb{R}^2$ is the geometric center of P_t . A new circle (or the original

shape) covering visible propagated pixels is drawn for each propagated frame, preserving the visual prompt’s color and opacity. We use **alpha blending** ($\Phi(\cdot)$) to overlay the visual prompts $\{P_1, P_2, \dots, P_T\}$ onto the original video frames: $\mathcal{V}'_i = \Phi(\mathcal{V}_i, P_i)$, $\forall 1 \leq i \leq T$. \mathcal{V}'_i is then fed to multimodal large language model (MLLM) in the following stage.

Unlike mask pooling or region-based feature extraction, alpha blending avoids pooling out unstable features, especially for prompts like arrows or circles that may only partially overlap with target objects. Additionally, by blending prompts onto frames, the model can directly learn geometric relationships between prompts and objects, enhancing robustness in object referring.

Video-Language Input. Blended video frames \mathcal{V}' are processed using the pre-trained visual encoder from Qwen2.5-VL [3], which extracts visual features from T frames and projects them into embeddings $v_{\text{visual}} \in \mathbb{R}^{\frac{T}{2} \times \frac{H}{14} \times \frac{W}{14} \times D}$. Text input is tokenized and encoded into embeddings $v_{\text{text}} \in \mathbb{R}^{L_t \times D}$. The visual and text embeddings are then concatenated and fed into the LLM, enabling joint reasoning over visual and textual modalities for object-centric video understanding. For segmentation outputs, frames are additionally resized and encoded into dense feature maps $v_{\text{dense}} \in \mathbb{R}^{T \times H' \times W' \times C}$ using the Hiera-L [50] encoder from SAM2 [49] (omitted in Fig. 2 for simplicity), triggered when a <SEG> token is detected in the response.

Decoder for Language and Grounding. LLM generates a sequence of text tokens, in which we add a special token <SEG> for segmentation outputs. Specifically, we locate the <SEG> tokens in text output, and project the corresponding last layer’s hidden states into the embedding space of the SAM2 prompt encoder, which is denoted as $\mathbf{h} \in \mathbb{R}^C$.

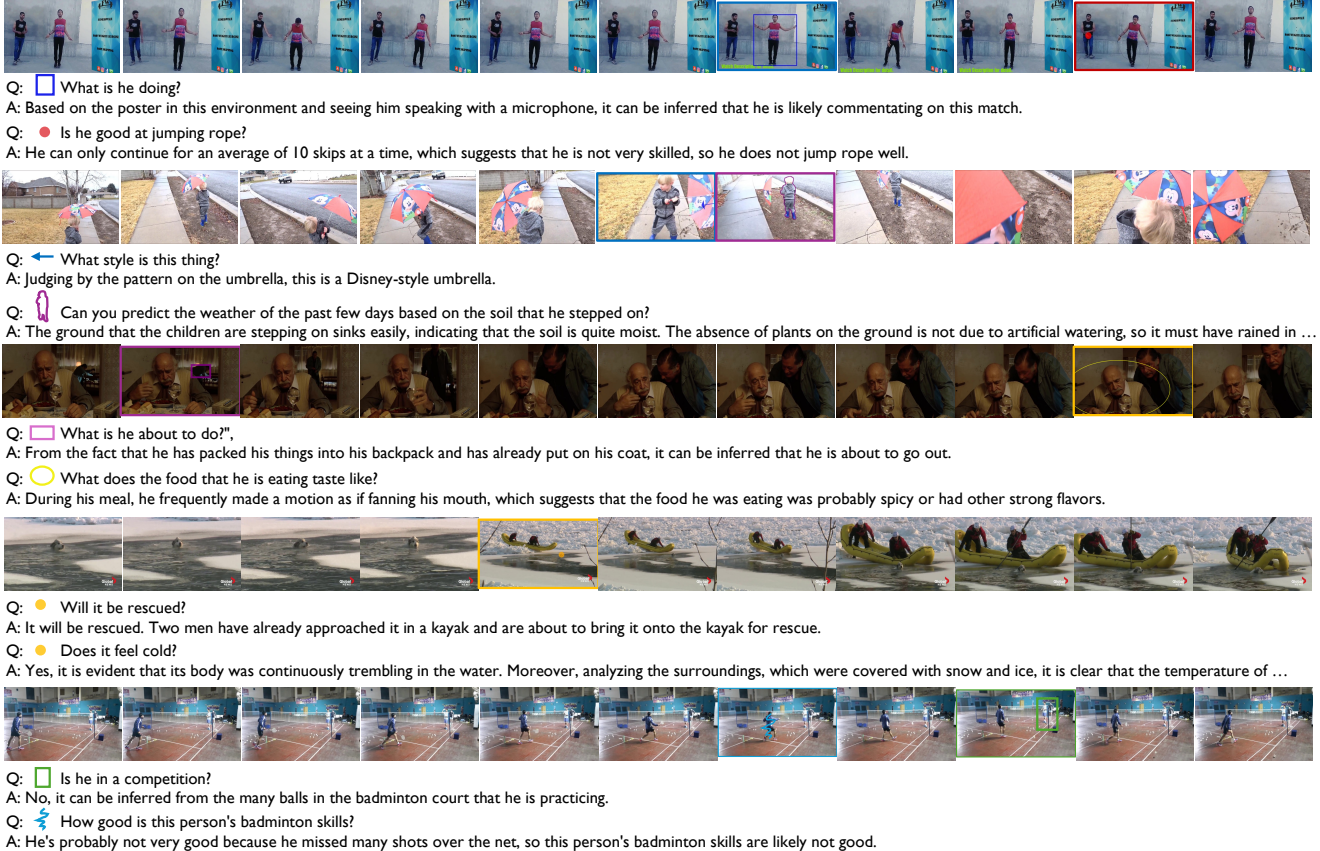


Figure 3. Visualization of samples in VideoInfer dataset. Some long answers have been truncated to accommodate width constraints.

The embedding \mathbf{h} are then passed to the SAM2 [49] decoder $\Psi_{\text{dec}}(\cdot)$ with dense visual feature maps v_{dense} , to produce the final segmentation masks $\mathcal{M} \in \mathbb{R}^{T \times H \times W}$:

$$\mathcal{M} = \Psi_{\text{dec}}(\mathbf{h}, v_{\text{dense}})$$

This integration allows the model to seamlessly combine language understanding and visual grounding, enabling joint reasoning and grounding outputs.

3.3. VideoInfer Dataset

This section presents the details of **VideoInfer**, a manually curated, object-centric video question-answering dataset, designed to challenge models with questions requiring semantic understanding, temporal reasoning, and instance discrimination over video content. Compared to existing object-level video question-answering datasets, which are often generated through automated pipelines, VideoInfer serves as a more rigorous benchmark for evaluating the reasoning capabilities of advanced VideoLLMs.

Dataset Collection. To construct VideoInfer, we curated 1,650 videos from diverse, high-quality object-centric video datasets, including TAO [2], LVOS [17], LVVIS [54], VIPSeg [41], UVO [56], MOSE [16], and OVIS [46], which

cover diverse scenarios such as indoor/outdoor activities, animal behaviors, and human interactions. These datasets provide dense mask annotations for objects that are used to automatically generate additional types of visual prompts, such as boxes, scribbles, and arrows following [7].

We prioritized long-form videos from TAO and LVOS for their rich, temporally dynamic content, making them ideal for crafting implicit reasoning questions. The original datasets provide masks or bounding boxes as annotations. We randomly generate 8 types of visual prompts (mask, mask contour, rectangle, ellipse, triangle, scribble, arrow, and point) based on mask annotations, and only prompt 1 frame for each video, to mimic the operations of the users. Each object with the visual prompt is manually annotated with question-answering (QA) pairs, following rules: **(i) indirectness:** the answer cannot be directly observed from the video but requires understanding and reasoning about the object of interest from users; or **(ii) dynamism:** questions require temporal reasoning, making it impossible to answer from a single frame. We apply cross-validation among two annotation groups, and low-scoring question-answer pairs are subsequently discarded.

Statistical Analysis. VideoInfer contains 1,620 videos and



Figure 4. Visualization of RGA3 results on VideoInfer dataset (zoom in for a better view).

28,811 QA pairs, split into two subsets: an instruction tuning set (950 videos with 2,555 objects and 20,320 QA pairs) and a challenging test set (670 videos with 1,572 objects and 8,491 QA pairs). This division provides a rigorous benchmark for evaluating future VideoLLMs. Visualizations of VideoInfer samples are provided in Fig. 3, most of the questions require inference and reasoning instead of directly observing the answer from the video. For example, in the first case, the question “Is he good at jumping rope?” requires the model to go through the entire video and analyze the actions of the man. Comparing with VideoRefer-700K [69], that contains automatically generated multiple-choice QA, our VideoInfer dataset contains open-ended questions that require deep reasoning.

3.4. Instruction Tuning

We finetune **RGA3** with a unified image-video training pipeline, treating images as single-frame videos to ensure smooth adaptation across both modalities. A complete list of training datasets is provided in Sec. 4.1. Since most existing Referring QA datasets provide only masks or bounding box annotations, we augment them by randomly generating different types of visual prompts during training. This data augmentation improves RGA3’s ability to handle diverse and arbitrary visual prompts effectively.

To enable both textual responses and segmentation outputs, we adopt a multi-task learning objective. Specifically, the text generation loss is defined as an autoregressive cross-entropy loss (\mathcal{L}_{txt}), while the segmentation loss ($\mathcal{L}_{\text{mask}}$) combines per-pixel binary cross-entropy (BCE) loss and DICE loss [42]. Given the ground-truth targets ($\hat{\mathbf{y}}_{\text{txt}}$, $\hat{\mathbf{m}}_{\text{tgt}}$) and the predictions (\mathbf{y}_{txt} , \mathbf{m}_{tgt}), the training ob-

jectives can be formulated as:

$$\mathcal{L}_{\text{txt}} = \text{CE}(\hat{\mathbf{y}}_{\text{txt}}, \mathbf{y}_{\text{txt}})$$

$$\mathcal{L}_{\text{mask}} = \lambda_{\text{bce}} \cdot \text{BCE}(\hat{\mathbf{m}}_{\text{tgt}}, \mathbf{m}_{\text{tgt}}) + \lambda_{\text{dice}} \cdot \text{DICE}(\hat{\mathbf{m}}_{\text{tgt}}, \mathbf{m}_{\text{tgt}})$$

The overall objective \mathcal{L} is the weighted sum of the text generation and segmentation losses: $\mathcal{L} = \lambda_{\text{txt}} \cdot \mathcal{L}_{\text{txt}} + \mathcal{L}_{\text{mask}}$.

4. Experiment

In this section, we first provide a detailed overview of the training datasets, implementation details, and evaluation metrics in Sec. 4.1. Then, we present extensive comparisons between RGA3 and state-of-the-art methods across a variety of visual QA and referring object segmentation benchmarks in Sec. 4.2. Finally, we conduct ablation studies to analyze the impact of STOM and SAM2 modules, indicating their contributions to overall performance in Sec. 4.3.

4.1. Experimental Setting

Training Datasets. The training datasets of RGA3 consist of two main parts: image/video QA datasets and image/video segmentation datasets. **(i)** We utilize various image-based QA datasets to improve the general question-answering capabilities, along with video-based QA datasets to foster temporal reasoning and inference; **(ii)** we include image/video segmentation datasets, which contain general semantic image segmentation datasets, and referring/reasoning object segmentation datasets to enable the grounding ability for RGA3. To enhance interactive visual reasoning, we mix both QA datasets and segmentation datasets during training. The detailed composition of the training datasets is listed in the Supplementary Material.

Method	BLEU-4 CIDEr ROUGE-L			GPT-4o
				(Acc. / Score)
<i>Generalist Models</i>				
VideoLLaMA3-7B [70]	4.1	48.0	21.2	39.1 / 2.28
Qwen2.5-VL-3B [3]	6.5	53.8	19.0	28.4 / 2.14
Qwen2.5-VL-7B [3]	6.4	54.6	23.8	41.7 / 2.42
GPT-4o (detail:low) [19]	7.6	62.7	22.9	44.1 / 2.48
GPT-4o (detail:high) [19]	7.6	64.4	23.0	45.5 / 2.50
<i>Specialist Models</i>				
Osprey-7B [68]	4.8	44.6	20.2	27.5 / 1.67
VideoRefer-7B [69]	7.4	77.8	25.6	40.4 / 2.29
RGA3-7B	12.2	104.3	29.9	46.7 / 2.60

Table 1. Evaluation of open-ended referring VideoQA task on our **VideoInfer** benchmark, given 8 different types of visual prompts. The ‘detail’ parameter adjusts the resolution of GPT-4o input.

Specifically, for the referring QA datasets, all the object references are initially annotated as masks or bounding boxes. We then randomly generate versatile visual prompts (mask, mask contour, rectangle, ellipse, triangle, scribble, arrow, and point) based on mask and bounding box annotations for both a single image and video frames, enabling more natural and flexible user interactions in instruction tuning. This visual prompt generation process is conducted on all referring QA datasets, including ViP-LLaVA-Instruct [7], Osprey-724K [68], and proposed VideoInfer.

Evaluation Metrics. We evaluate our model from two primary perspectives: Referring QA and Referring/Reasoning object segmentation at both the video-level and image-level. (i) For video Referring QA, we report accuracy on multiple-choice questions on VideoRefer-Bench^Q [69]. On our VideoInfer benchmark, we adopt BLEU-4 [43], CIDEr [53], ROUGE-L [34] and GPT-4o evaluated accuracy / score [39] as metrics for open-ended questions, following previous works [14, 39]. For image Referring QA, we follow the official GPT-4-turbo-based evaluation on ViP-Bench [7], averaging results over 5 runs. (ii) For Referring/Reasoning video object segmentation, we adopt region similarity (\mathcal{J}), contour accuracy (\mathcal{F}), and their average ($\mathcal{J}\&\mathcal{F}$), consistent with prior methods. The robustness score (\mathcal{R}) [31] is adopted to evaluate hallucinations on ReVOS [60].

Implementation Details. Our proposed RGA3 model is implemented with Qwen2.5-VL-7B [3] as the visual-language backbone and SAM2 (Hiera-L) [49, 50] as the grounding module by default. The training is conducted on 16 NVIDIA H800 (80GB) GPUs distributed across 2 nodes, with a batch size of 2 per device and gradient accumulation steps set to 8, leading to a total of 256 effective samples per update. We utilize the DeepSpeed engine to manage distributed training and optimization efficiently. The optimization process employs the AdamW optimizer [38], combined with a WarmupCosineLR learning rate scheduler. The

Method	Input	Basic	Seq.	Rel.	Rea.	Pred.	Avg.
<i>Generalist Models</i>							
Qwen2-VL-7B [55]	SoM	62.0	69.6	54.9	87.3	74.6	66.0
InternVL2-26B [11]	SoM	58.5	63.5	53.4	88.0	78.9	65.0
GPT-4o-mini [19]	SoM	57.6	67.1	56.5	85.9	75.4	65.8
GPT-4o [19]	SoM	62.3	74.5	66.0	88.0	73.7	71.3
<i>Specialist Models</i>							
Osprey-7B [68]	RF	45.9	47.1	30.0	48.6	23.7	39.9
Ferret-7B [65]	RF	35.2	44.7	41.9	70.4	74.6	48.8
VideoRefer-7B [69]	RF	75.4	68.6	59.3	89.4	78.1	71.9
RGA3-7B (Ours)	VP	77.4	71.9	61.1	88.8	81.6	74.0

Table 2. Evaluation of multiple-choice referring VideoQA task on **VideoRefer-Bench^Q** [69], given different object referring approaches. ‘SoM’, ‘RF’, and ‘VP’ represent Set-of-Mask [62], region feature, and visual prompt, respectively.

Method	Format	Synthesized	Manual
GPT-4V-turbo (detail: high) [1]	VP	60.7	59.9
GPT-4V-turbo (detail: low) [1]	VP	52.8	51.4
Shikra-7B [8]	Coor	33.7	–
GPT4ROI-7B [73]	ROI	35.1	–
Kosmos-2 [45]	Dis	26.9	–
ViP-LLaVA-Base-13B [7]	VP	48.2	47.0
ViP-LLaVA-13B [7]	VP	48.3	48.2
RGA3-7B (Ours)	VP	48.7	49.4

Table 3. Evaluation of image-level referring QA task on **ViP-Bench** [7], given eight different types of visual prompts.

maximum learning rate is set to 4×10^{-5} , with a gradual warm-up phase to stabilize initial training dynamics. We assign the loss weights for the next token prediction loss, binary cross-entropy (BCE) loss, and DICE loss as 1.0, 2.0, and 0.5, respectively, ensuring a balanced training objective for both text generation and segmentation mask prediction. Throughout the training process, the visual encoders remain frozen to preserve pre-trained visual knowledge, while the LLM is fine-tuned using LoRA [18], enabling efficient and memory-friendly adaptation of the model parameters.

4.2. Comparison

Referring Question Answering. We evaluate RGA3 on both image and video-level referring QA datasets, including VideoInfer (Ours), VideoRefer-Bench^Q [69], and ViP-Bench [7]. The performance comparison on VideoInfer is presented in Tab. 1. As shown, RGA3 outperforms the concurrent work VideoRefer [69] by 6.3/0.31 in terms of GPT-4o evaluated accuracy/score, demonstrating its strong ability in video reasoning and object-centric understanding under various visual prompts. As VideoInfer contains different types of visual prompts instead of pure masks as object referring inputs, this comparison indicates the strong abil-

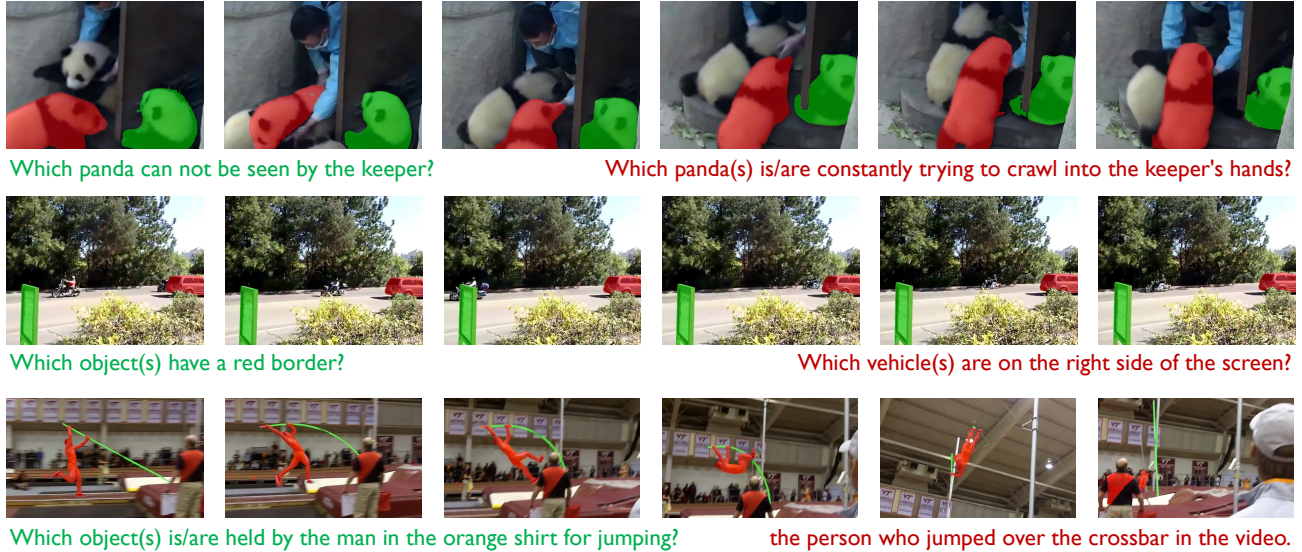


Figure 5. Visualization of the RGA3 grounding results on ReVOS dataset.

Method	ReasonVOS [4]			ReVOS [60]									
	$\mathcal{J}\&\mathcal{F}$	\mathcal{J}	\mathcal{F}	overall			referring			reasoning			\mathcal{R}
				$\mathcal{J}\&\mathcal{F}$	\mathcal{J}	\mathcal{F}	$\mathcal{J}\&\mathcal{F}$	\mathcal{J}	\mathcal{F}	$\mathcal{J}\&\mathcal{F}$	\mathcal{J}	\mathcal{F}	
LISA-7B [26]	31.1	29.1	33.1	40.9	39.1	42.7	45.7	44.3	47.1	36.1	33.8	38.4	9.3
VISA-7B [60]	-	-	-	46.9	44.9	49.0	50.9	49.2	52.6	43.0	40.6	45.4	15.5
VideoLISA-3.8B [4]	45.1	43.1	47.1	48.4	46.1	50.7	53.0	51.0	55.1	43.8	41.2	46.4	20.1
RGA3-3B (Ours)	51.7	49.1	54.3	56.1	54.1	58.0	59.3	57.6	61.0	52.8	50.6	55.0	27.7
RGA3-7B (Ours)	53.6	51.3	56.0	58.0	55.9	60.0	60.5	58.7	62.3	55.4	53.1	57.7	28.6

Table 4. Comparison on video-level reasoning object segmentation datasets.

ity of RGA3 to process arbitrary visual prompts, and thus being more interactive friendly.

Results in Tab. 2 show that RGA3 achieves state-of-the-art performance across both image-level and video-level referring QA tasks. Specifically, RGA3-7B surpasses the best region feature-based method VideoRefer-7B [69] by 2.1% and exceeds the SoM-based GPT-4o method by 2.7% on the VideoRefer-Bench^Q dataset. As shown in Tab. 3, without being specifically designed for image-level tasks, RGA3 achieves comparable performance with ViP-LLaVA-13B models [7] on ViP-Bench [7] for image-level referring QA with diverse visual prompt types. The visualization of RGA3 on the VideoInfer benchmark is shown in Fig. 4.

Referring & Reasoning Segmentation. As shown in Tab. 4 and Tab. 5, RGA3 significantly outperforms the existing state-of-the-art video object segmentation models across multiple benchmarks. Specifically, RGA3-7B surpasses state-of-the-art MLLM-based methods VISA [60] and VideoLISA [4] by around 10% on both the ReasonVOS [4] and ReVOS [60] datasets, demonstrating its superior reasoning-based video object segmentation ability. On general referring video object segmentation datasets,

including MeVIS [15], Ref-Youtube-VOS [51], and Ref-DAVIS-17 [22], RGA3 consistently outperforms existing VideoLLMs (VideoLISA [4], VISA [60]) and image-level MLLMs such as LISA [26], highlighting its robust grounding capability across diverse video segmentation datasets. The visualization results of RGA3 on the video reasoning segmentation benchmark are presented in Fig. 5. Moreover, RGA3 outperforms state-of-the-art MLLM-based methods on image-level segmentation benchmarks including Ref-COCO(+g) [21, 40] and ReasonSeg [26], demonstrating the general grounding ability of RGA3 on image-level grounding tasks. The detailed results on image segmentation benchmarks are shown in the Supplementary Material.

In summary, our proposed RGA3 achieves state-of-the-art performance in both video referring QA and video referring/reasoning object segmentation tasks, enabling multi-modal processing in both model inputs and outputs. This advancement enhances user interaction by supporting multi-round and multi-modal conversational object-centric reasoning on videos.

Method	MeViS <i>val^u</i> [15]			MeViS <i>val</i> [15]			Ref-YouTube-VOS [51]			Ref-DAVIS-17 [22]		
	$\mathcal{J}\&\mathcal{F}$	\mathcal{J}	\mathcal{F}	$\mathcal{J}\&\mathcal{F}$	\mathcal{J}	\mathcal{F}	$\mathcal{J}\&\mathcal{F}$	\mathcal{J}	\mathcal{F}	$\mathcal{J}\&\mathcal{F}$	\mathcal{J}	\mathcal{F}
LISA-7B [26]	44.8	41.1	48.6	37.2	35.1	39.4	50.2	49.7	50.6	58.4	54.9	61.9
VISA-7B [60]	-	-	-	43.5	40.7	46.3	61.5	59.8	63.2	69.4	66.3	72.5
VideoLISA-3.8B [4]	51.7	48.4	57.9	44.4	41.3	47.6	61.7	60.2	63.3	67.7	63.8	71.5
RGA3-3B (Ours)	57.7	54.7	60.7	48.8	46.2	51.5	67.4	65.8	69.1	72.1	67.6	76.6
RGA3-7B (Ours)	59.7	56.7	62.6	50.1	47.4	52.8	68.5	66.8	70.1	72.8	68.3	77.3

Table 5. Comparison on video-level referring object segmentation datasets. All comparisons on segmentation tasks are conducted under the same end-to-end manner without extra post-optimization methods such as XMem [12] or XMem++ [5].

4.3. Ablation Studies

Ablation of the proposed STOM module. In Tab. 6, we investigate the effectiveness of STOM. The region feature-based approach computes average pixel features through mask pooling, which serves as a common strategy for region-level reasoning. However, an arrow or scribble pointing to an object may only partially overlap with the object of interest, leading to a noisy and incomplete object feature. To overcome this limitation, we adopt an overlay-based approach that directly integrates visual prompts with original frames, allowing the model to learn end-to-end geometric relationships between different visual prompt types and their corresponding objects. As shown, RGA3 w/o STOM achieves 43.6/2.46 on the VideoInfer dataset. By incorporating tracking and overlaying, RGA3 w/ STOM achieves 46.7/2.60, demonstrating the effectiveness of our overlay-based approach for spatial-temporal prompt reasoning. The oracle propagation in the last row refers to the use of ground truth masks to generate consistent visual prompts for all frames as the object reference.

Ablation of the segmentation module. As shown in Tab. 7, RGA3-7B with the SAM decoder [23] already outperforms VISA-7B [60] (which uses the same SAM decoder) by 8.5 and 15.7 on the ReVOS and ReasonSeg benchmarks, respectively. Incorporating SAM2 provides a 2.6 improvement on ReVOS [60] and a marginal gain on ReasonSeg [26] compared to the SAM decoder, suggesting that RGA3’s segmentation performance improvements stem primarily from its comprehensive video content understanding and memory attention mechanism.

We also provide the latency and memory usage of the STOM and SAM2 module on 1K samples of VideoRefer-Bench^Q / ReVOS with one H800 (80G) in tab. 8. We find that the propagation process of SAM2 and the tracking process of CoTracker3 cost most time, except for the forward process of LLM.

5. Conclusion

In this work, we introduce RGA3, a multi-modal interactive VideoLLM that unifies video referring and grounding tasks

Method	VideoRefer-Bench ^Q (16)	VideoInfer (8)
	Acc.	Acc. / Score
w/o STOM	72.2	43.6 / 2.46
w/ STOM	74.0	46.7 / 2.60
w/ oracle prop.	75.1	44.8 / 2.52

Table 6. Ablation on propagating visual prompts across the remaining frames. (16) represents 16 frames as input for inference.

Method	ReVOS [60]			ReasonSeg _{val} [26]	
	$\mathcal{J}\&\mathcal{F}$	\mathcal{J}	\mathcal{F}	gIoU	cIoU
LISA-7B [26]	40.9	39.1	42.7	52.9	54.0
VISA-7B [60]	46.9	44.9	49.0	52.7	57.8
VideoLISA-3.8B [4]	48.4	46.1	50.7	61.4	67.1
RGA3-7B-SAM	55.4	53.4	57.4	68.5	68.6
RGA3-7B-SAM2	58.0	55.9	60.0	68.7	70.2

Table 7. Comparison on the choice of the grounding module.

Component	Latency (s/sample)	FPS	Memory
STOM	0.483	43.0	3.8G
SAM2 (Hiera-L)	4.543	35.6	5.4G

Table 8. Latency and memory usage of STOM and SAM2.

in a multi-round conversational manner. By incorporating the Spatial-Temporal Overlay Module (STOM), our model effectively processes versatile visual prompts at any timestamp, enhancing user interaction and fine-grained object reasoning in videos. Furthermore, we introduce VideoInfer, a manually curated video instruction dataset designed to challenge Video LLMs with deep reasoning and inference-based question-answering, surpassing existing datasets in complexity and reasoning depth. Through extensive evaluations across VideoInfer as well as 11 existing benchmarks, we demonstrate the superior performance of RGA3 in both referring question-answering and reasoning-based segmentation tasks. We publicly release our dataset, code, and web demo to facilitate future advancements in video understanding. We hope that RGA3 and VideoInfer will serve as a strong foundation for future research, pushing the boundaries of object-centric video comprehension.

References

- [1] Josh Achiam, Steven Adler, Sandhini Agarwal, Lama Ahmad, Ilge Akkaya, Florencia Leoni Aleman, Diogo Almeida, Janko Altenschmidt, Sam Altman, Shyamal Anadkat, et al. Gpt-4 technical report. *arXiv preprint arXiv:2303.08774*, 2023. 6
- [2] Ali Athar, Jonathon Luiten, Paul Voigtlaender, Tarasha Khurana, Achal Dave, Bastian Leibe, and Deva Ramanan. Burst: A benchmark for unifying object recognition, segmentation and tracking in video. In *Proceedings of the IEEE/CVF Winter Conference on Applications of Computer Vision*, pages 1674–1683, 2023. 4
- [3] Shuai Bai, Keqin Chen, Xuejing Liu, Jialin Wang, Wenbin Ge, Sibao Song, Kai Dang, Peng Wang, Shijie Wang, Jun Tang, Humen Zhong, Yanzhi Zhu, Mingkun Yang, Zhaohai Li, Jianqiang Wan, Pengfei Wang, Wei Ding, Zheren Fu, Yiheng Xu, Jiabo Ye, Xi Zhang, Tianbao Xie, Zesen Cheng, Hang Zhang, Zhibo Yang, Haiyang Xu, and Junyang Lin. Qwen2.5-vl technical report. *arXiv preprint arXiv:2502.13923*, 2025. 3, 6, 1
- [4] Zechen Bai, Tong He, Haiyang Mei, Pichao Wang, Ziteng Gao, Joya Chen, Zheng Zhang, and Mike Zheng Shou. One token to seg them all: Language instructed reasoning segmentation in videos. *Advances in Neural Information Processing Systems*, 37:6833–6859, 2024. 2, 7, 8, 1
- [5] Maksym Bekuzarov, Ariana Bermudez, Joon-Young Lee, and Hao Li. Xmem++: Production-level video segmentation from few annotated frames. In *Proceedings of the IEEE/CVF International Conference on Computer Vision (CVPR)*, pages 635–644, 2023. 8
- [6] Holger Caesar, Jasper Uijlings, and Vittorio Ferrari. Coco-stuff: Thing and stuff classes in context. In *Proceedings of the IEEE Conference on Computer Vision and Pattern Recognition (CVPR)*, pages 1209–1218, 2018. 1
- [7] Mu Cai, Haotian Liu, Siva Karthik Mustikovela, Gregory P Meyer, Yuning Chai, Dennis Park, and Yong Jae Lee. Vip-llava: Making large multi-modal models understand arbitrary visual prompts. In *Proceedings of the IEEE/CVF Conference on Computer Vision and Pattern Recognition (CVPR)*, pages 12914–12923, 2024. 4, 6, 7, 1
- [8] Keqin Chen, Zhao Zhang, Weili Zeng, Richong Zhang, Feng Zhu, and Rui Zhao. Shikra: Unleashing multimodal llm’s referential dialogue magic. *arXiv preprint arXiv:2306.15195*, 2023. 6
- [9] Qirui Chen, Shangzhe Di, and Weidi Xie. Grounded multi-hop videoqa in long-form egocentric videos. *arXiv preprint arXiv:2408.14469*, 2024. 1
- [10] Xianjie Chen, Roozbeh Mottaghi, Xiaobai Liu, Sanja Fidler, Raquel Urtasun, and Alan Yuille. Detect what you can: Detecting and representing objects using holistic models and body parts. In *Proceedings of the IEEE Conference on Computer Vision and Pattern Recognition (CVPR)*, pages 1971–1978, 2014. 1
- [11] Zhe Chen, Weiyun Wang, Hao Tian, Shenglong Ye, Zhangwei Gao, Erfei Cui, Wenwen Tong, Kongzhi Hu, Jiapeng Luo, Zheng Ma, et al. How far are we to gpt-4v? closing the gap to commercial multi-modal models with open-source suites. *arXiv preprint arXiv:2404.16821*, 2024. 6
- [12] Ho Kei Cheng and Alexander G Schwing. Xmem: Long-term video object segmentation with an atkinson-shiffrin memory model. In *European Conference on Computer Vision (ECCV)*, pages 640–658. Springer, 2022. 8
- [13] Zesen Cheng, Sicong Leng, Hang Zhang, Yifei Xin, Xin Li, Guanzheng Chen, Yongxin Zhu, Wenqi Zhang, Ziyang Luo, Deli Zhao, et al. Videollama 2: Advancing spatial-temporal modeling and audio understanding in video-llms. *arXiv preprint arXiv:2406.07476*, 2024. 1
- [14] Shangzhe Di and Weidi Xie. Grounded question-answering in long egocentric videos. In *Proceedings of the IEEE/CVF Conference on Computer Vision and Pattern Recognition (CVPR)*, pages 12934–12943, 2024. 1, 6
- [15] Henghui Ding, Chang Liu, Shuting He, Xudong Jiang, and Chen Change Loy. Mevis: A large-scale benchmark for video segmentation with motion expressions. In *Proceedings of the IEEE/CVF International Conference on Computer Vision (ICCV)*, pages 2694–2703, 2023. 7, 8, 1
- [16] Henghui Ding, Chang Liu, Shuting He, Xudong Jiang, Philip HS Torr, and Song Bai. Mose: A new dataset for video object segmentation in complex scenes. In *Proceedings of the IEEE/CVF International Conference on Computer Vision (ICCV)*, pages 20224–20234, 2023. 4
- [17] Lingyi Hong, Zhongying Liu, Wenchao Chen, Chenzhi Tan, Yuang Feng, Xinyu Zhou, Pinxue Guo, Jinglun Li, Zhaoyu Chen, Shuyong Gao, et al. Lvos: A benchmark for large-scale long-term video object segmentation. *arXiv preprint arXiv:2404.19326*, 2024. 4
- [18] Edward J Hu, Yelong Shen, Phillip Wallis, Zeyuan Allen-Zhu, Yanzhi Li, Shean Wang, Lu Wang, and Weizhu Chen. Lora: Low-rank adaptation of large language models. *arXiv preprint arXiv:2106.09685*, 2021. 6
- [19] Aaron Hurst, Adam Lerer, Adam P Goucher, Adam Perelman, Aditya Ramesh, Aidan Clark, AJ Ostrow, Akila Welihinda, Alan Hayes, Alec Rad-

- ford, et al. Gpt-4o system card. *arXiv preprint arXiv:2410.21276*, 2024. 6
- [20] Nikita Karaev, Iurii Makarov, Jianyuan Wang, Natalia Neverova, Andrea Vedaldi, and Christian Rupprecht. Cotracker3: Simpler and better point tracking by pseudo-labelling real videos. In *Proceedings of the IEEE/CVF International Conference on Computer Vision (ICCV)*, 2025. 3
- [21] Sahar Kazemzadeh, Vicente Ordonez, Mark Matten, and Tamara Berg. Referitgame: Referring to objects in photographs of natural scenes. In *Proceedings of the 2014 Conference on Empirical Methods in Natural Language Processing (EMNLP)*, pages 787–798, 2014. 7, 1, 2
- [22] Anna Khoreva, Anna Rohrbach, and Bernt Schiele. Video object segmentation with language referring expressions. In *Computer Vision—ACCV 2018: 14th Asian Conference on Computer Vision, Perth, Australia, December 2–6, 2018, Revised Selected Papers, Part IV 14*, pages 123–141. Springer, 2019. 7, 8, 1
- [23] Alexander Kirillov, Eric Mintun, Nikhila Ravi, Hanzi Mao, Chloe Rolland, Laura Gustafson, Tete Xiao, Spencer Whitehead, Alexander C Berg, Wan-Yen Lo, et al. Segment anything. In *Proceedings of the IEEE/CVF International Conference on Computer Vision (ICCV)*, pages 4015–4026, 2023. 8
- [24] Jing Yu Koh, Ruslan Salakhutdinov, and Daniel Fried. Grounding language models to images for multimodal inputs and outputs. In *International Conference on Machine Learning*, pages 17283–17300. PMLR, 2023. 2
- [25] Jing Yu Koh, Daniel Fried, and Russ R Salakhutdinov. Generating images with multimodal language models. *Advances in Neural Information Processing Systems*, 36, 2024. 2
- [26] Xin Lai, Zhuotao Tian, Yukang Chen, Yanwei Li, Yuhui Yuan, Shu Liu, and Jiaya Jia. Lisa: Reasoning segmentation via large language model. In *Proceedings of the IEEE/CVF Conference on Computer Vision and Pattern Recognition (CVPR)*, pages 9579–9589, 2024. 7, 8, 1, 2
- [27] Bo Li, Yuanhan Zhang, Liangyu Chen, Jinghao Wang, Fanyi Pu, Jingkang Yang, Chunyuan Li, and Ziwei Liu. Mimic-it: Multi-modal in-context instruction tuning. *arXiv preprint arXiv:2306.05425*, 2023. 2
- [28] Bo Li, Yuanhan Zhang, Dong Guo, Renrui Zhang, Feng Li, Hao Zhang, Kaichen Zhang, Peiyuan Zhang, Yanwei Li, Ziwei Liu, et al. Llava-onevision: Easy visual task transfer. *arXiv preprint arXiv:2408.03326*, 2024. 2, 1
- [29] Feng Li, Renrui Zhang, Hao Zhang, Yuanhan Zhang, Bo Li, Wei Li, Zejun Ma, and Chunyuan Li. Llava-next-interleave: Tackling multi-image, video, and 3d in large multimodal models. *arXiv preprint arXiv:2407.07895*, 2024. 2
- [30] Kunchang Li, Yali Wang, Yinan He, Yizhuo Li, Yi Wang, Yi Liu, Zun Wang, Jilan Xu, Guo Chen, Ping Luo, et al. Mvbench: A comprehensive multi-modal video understanding benchmark. In *Proceedings of the IEEE Conference on Computer Vision and Pattern Recognition (CVPR)*, pages 22195–22206, 2024. 1
- [31] Xiang Li, Jinglu Wang, Xiaohao Xu, Xiao Li, Bhiksha Raj, and Yan Lu. Towards robust referring video object segmentation with cyclic relational consensus. *arXiv preprint arXiv:2207.01203*, 2022. 6
- [32] Long Lian, Yifan Ding, Yunhao Ge, Sifei Liu, Hanzi Mao, Boyi Li, Marco Pavone, Ming-Yu Liu, Trevor Darrell, Adam Yala, and Yin Cui. Describe anything: Detailed localized image and video captioning. In *Proceedings of the IEEE/CVF International Conference on Computer Vision (ICCV)*, 2025. 2
- [33] Bin Lin, Yang Ye, Bin Zhu, Jiayi Cui, Munan Ning, Peng Jin, and Li Yuan. Video-llava: Learning united visual representation by alignment before projection. *arXiv preprint arXiv:2311.10122*, 2023. 1, 2
- [34] Chin-Yew Lin. Rouge: A package for automatic evaluation of summaries. In *Text Summarization Branches Out*, pages 74–81, 2004. 6
- [35] Lang Lin, Xueyang Yu, Ziqi Pang, and Yu-Xiong Wang. Glus: Global-local reasoning unified into a single large language model for video segmentation. In *Proceedings of the IEEE Conference on Computer Vision and Pattern Recognition (CVPR)*, 2025. 2
- [36] Haotian Liu, Chunyuan Li, Qingyang Wu, and Yong Jae Lee. Visual instruction tuning. *Advances in Neural Information Processing Systems*, 36, 2024. 2, 1
- [37] Yikun Liu, Pingan Chen, Jiayin Cai, Xiaolong Jiang, Yao Hu, Jiangchao Yao, Yanfeng Wang, and Weidi Xie. Lamra: Large multimodal model as your advanced retrieval assistant. In *Proceedings of the IEEE/CVF Conference on Computer Vision and Pattern Recognition (CVPR)*, 2025. 2
- [38] Ilya Loshchilov and Frank Hutter. Decoupled weight decay regularization. *arXiv preprint arXiv:1711.05101*, 2017. 6
- [39] Muhammad Maaz, Hanoona Rasheed, Salman Khan, and Fahad Shahbaz Khan. Video-chatgpt: Towards detailed video understanding via large vision and language models. *arXiv preprint arXiv:2306.05424*, 2023. 6, 1
- [40] Junhua Mao, Jonathan Huang, Alexander Toshev, Oana Camburu, Alan L Yuille, and Kevin Murphy. Generation and comprehension of unambiguous object descriptions. In *Proceedings of the IEEE Con-*

- ference on Computer Vision and Pattern Recognition (CVPR)*, pages 11–20, 2016. [7](#), [1](#), [2](#)
- [41] Jiayu Miao, Xiaohan Wang, Yu Wu, Wei Li, Xu Zhang, Yunchao Wei, and Yi Yang. Large-scale video panoptic segmentation in the wild: A benchmark. In *Proceedings of the IEEE/CVF Conference on Computer Vision and Pattern Recognition (CVPR)*, pages 21033–21043, 2022. [4](#)
- [42] Fausto Milletari, Nassir Navab, and Seyed-Ahmad Ahmadi. V-net: Fully convolutional neural networks for volumetric medical image segmentation. In *2016 Fourth International Conference on 3D Vision*, pages 565–571. IEEE, 2016. [5](#)
- [43] Kishore Papineni, Salim Roukos, Todd Ward, and Wei-Jing Zhu. Bleu: A method for automatic evaluation of machine translation. In *Proceedings of the 40th Annual Meeting of the Association for Computational Linguistics*, pages 311–318, 2002. [6](#)
- [44] Viorica Patraucean, Lucas Smaira, Ankush Gupta, Adria Recasens, Larisa Markeeva, Dylan Banarse, Skanda Koppula, Mateusz Malinowski, Yi Yang, Carl Doersch, et al. Perception test: A diagnostic benchmark for multimodal video models. *Advances in Neural Information Processing Systems*, 36:42748–42761, 2023. [1](#)
- [45] Zhiliang Peng, Wenhui Wang, Li Dong, Yaru Hao, Shaohan Huang, Shuming Ma, and Furu Wei. Kosmos-2: Grounding multimodal large language models to the world. *arXiv preprint arXiv:2306.14824*, 2023. [6](#)
- [46] Jiyang Qi, Yan Gao, Yao Hu, Xinggang Wang, Xiaoyu Liu, Xiang Bai, Serge Belongie, Alan Yuille, Philip HS Torr, and Song Bai. Occluded video instance segmentation: A benchmark. *International Journal of Computer Vision*, 130(8):2022–2039, 2022. [4](#)
- [47] Jihao Qiu, Yuan Zhang, Xi Tang, Lingxi Xie, Tianren Ma, Pengyu Yan, David Doermann, Qixiang Ye, and Yunjie Tian. Artemis: Towards referential understanding in complex videos. In *The Thirty-eighth Annual Conference on Neural Information Processing Systems*, 2024. [1](#)
- [48] Vignesh Ramanathan, Anmol Kalia, Vladan Petrovic, Yi Wen, Baixue Zheng, Baishan Guo, Rui Wang, Aaron Marquez, Rama Kovvuri, Abhishek Kadian, et al. Paco: Parts and attributes of common objects. In *Proceedings of the IEEE/CVF Conference on Computer Vision and Pattern Recognition (CVPR)*, pages 7141–7151, 2023. [1](#)
- [49] Nikhila Ravi, Valentin Gabeur, Yuan-Ting Hu, Ronghang Hu, Chaitanya Ryali, Tengyu Ma, Haitham Khedr, Roman Rädle, Chloe Rolland, Laura Gustafson, et al. Sam 2: Segment anything in images and videos. *arXiv preprint arXiv:2408.00714*, 2024. [2](#), [3](#), [4](#), [6](#)
- [50] Chaitanya Ryali, Yuan-Ting Hu, Daniel Bolya, Chen Wei, Haoqi Fan, Po-Yao Huang, Vaibhav Aggarwal, Arkabandhu Chowdhury, Omid Poursaeed, Judy Hoffman, et al. Hiera: A hierarchical vision transformer without the bells-and-whistles. In *International Conference on Machine Learning*, pages 29441–29454. PMLR, 2023. [3](#), [6](#)
- [51] Seonguk Seo, Joon-Young Lee, and Bohyung Han. Urvos: Unified referring video object segmentation network with a large-scale benchmark. In *European Conference on Computer Vision (ECCV)*, pages 208–223. Springer, 2020. [7](#), [8](#), [1](#)
- [52] Quan Sun, Qiyang Yu, Yufeng Cui, Fan Zhang, Xiaosong Zhang, Yueze Wang, Hongcheng Gao, Jingjing Liu, Tiejun Huang, and Xinlong Wang. Generative pretraining in multimodality. *arXiv preprint arXiv:2307.05222*, 2023. [2](#)
- [53] Ramakrishna Vedantam, C Lawrence Zitnick, and Devi Parikh. Cider: Consensus-based image description evaluation. In *Proceedings of the IEEE conference on Computer Vision and Pattern Recognition (CVPR)*, pages 4566–4575, 2015. [6](#)
- [54] Haochen Wang, Cilin Yan, Keyan Chen, Xiaolong Jiang, Xu Tang, Yao Hu, Guoliang Kang, Weidi Xie, and Efstratios Gavves. Ov-vis: Open-vocabulary video instance segmentation. *International Journal of Computer Vision*, pages 1–18, 2024. [4](#)
- [55] Peng Wang, Shuai Bai, Sinan Tan, Shijie Wang, Zhihao Fan, Jinze Bai, Keqin Chen, Xuejing Liu, Jialin Wang, Wenbin Ge, et al. Qwen2-vl: Enhancing vision-language model’s perception of the world at any resolution. *arXiv preprint arXiv:2409.12191*, 2024. [6](#)
- [56] Weiyao Wang, Matt Feiszli, Heng Wang, and Du Tran. Unidentified video objects: A benchmark for dense, open-world segmentation. In *Proceedings of the IEEE/CVF International Conference on Computer Vision (ICCV)*, pages 10776–10785, 2021. [4](#)
- [57] Yi Wang, Kunchang Li, Yizhuo Li, Yinan He, Bingkun Huang, Zhiyu Zhao, Hongjie Zhang, Jilan Xu, Yi Liu, Zun Wang, et al. Internvideo: General video foundation models via generative and discriminative learning. *arXiv preprint arXiv:2212.03191*, 2022. [2](#)
- [58] Yi Wang, Kunchang Li, Xinhao Li, Jiashuo Yu, Yinan He, Guo Chen, Baoqi Pei, Rongkun Zheng, Zun Wang, Yansong Shi, et al. Internvideo2: Scaling foundation models for multimodal video understanding. In *European Conference on Computer Vision (ECCV)*, pages 396–416. Springer, 2024. [2](#)

- [59] Junbin Xiao, Xindi Shang, Angela Yao, and Tat-Seng Chua. Next-qa: Next phase of question-answering to explaining temporal actions. In *Proceedings of the IEEE Conference on Computer Vision and Pattern Recognition (CVPR)*, pages 9777–9786, 2021. 1
- [60] Cilin Yan, Haochen Wang, Shilin Yan, Xiaolong Jiang, Yao Hu, Guoliang Kang, Weidi Xie, and Efstathios Gavves. Visa: Reasoning video object segmentation via large language models. In *European Conference on Computer Vision (ECCV)*, pages 98–115. Springer, 2024. 2, 6, 7, 8, 1
- [61] Wilson Yan, Yunzhi Zhang, Pieter Abbeel, and Aravind Srinivas. Videogpt: Video generation using vq-vae and transformers. *arXiv preprint arXiv:2104.10157*, 2021. 1, 2
- [62] Jianwei Yang, Hao Zhang, Feng Li, Xueyan Zou, Chunyuan Li, and Jianfeng Gao. Set-of-mark prompting unleashes extraordinary visual grounding in gpt-4v. *arXiv preprint arXiv:2310.11441*, 2023. 6
- [63] Senqiao Yang, Tianyuan Qu, Xin Lai, Zhuotao Tian, Bohao Peng, Shu Liu, and Jiaya Jia. Lisa++: An improved baseline for reasoning segmentation with large language model. *arXiv preprint arXiv:2312.17240*, 2023. 1
- [64] Qinghao Ye, Haiyang Xu, Guohai Xu, Jiabo Ye, Ming Yan, Yiyang Zhou, Junyang Wang, Anwen Hu, Pengcheng Shi, Yaya Shi, et al. mplug-owl: Modularization empowers large language models with multimodality. *arXiv preprint arXiv:2304.14178*, 2023. 2
- [65] Haoxuan You, Haotian Zhang, Zhe Gan, Xianzhi Du, Bowen Zhang, Zirui Wang, Liangliang Cao, Shih-Fu Chang, and Yinfei Yang. Ferret: Refer and ground anything anywhere at any granularity. *arXiv preprint arXiv:2310.07704*, 2023. 2, 6
- [66] Zhou Yu, Dejing Xu, Jun Yu, Ting Yu, Zhou Zhao, Yueting Zhuang, and Dacheng Tao. Activitynet-qa: A dataset for understanding complex web videos via question answering. In *Proceedings of the AAAI Conference on Artificial Intelligence*, pages 9127–9134, 2019. 1
- [67] Haobo Yuan, Xiangtai Li, Tao Zhang, Zilong Huang, Shilin Xu, Shunping Ji, Yunhai Tong, Lu Qi, Jiashi Feng, and Ming-Hsuan Yang. Sa2va: Marrying sam2 with llava for dense grounded understanding of images and videos. *arXiv*, 2025. 2
- [68] Yuqian Yuan, Wentong Li, Jian Liu, Dongqi Tang, Xinjie Luo, Chi Qin, Lei Zhang, and Jianke Zhu. Osprey: Pixel understanding with visual instruction tuning. In *Proceedings of the IEEE/CVF Conference on Computer Vision and Pattern Recognition (CVPR)*, pages 28202–28211, 2024. 2, 6, 1
- [69] Yuqian Yuan, Hang Zhang, Wentong Li, Zesen Cheng, Boqiang Zhang, Long Li, Xin Li, Deli Zhao, Wenqiao Zhang, Yueting Zhuang, et al. Videorefer suite: Advancing spatial-temporal object understanding with video llm. In *Proceedings of the IEEE/CVF Conference on Computer Vision and Pattern Recognition (CVPR)*, 2025. 2, 5, 6, 7, 1
- [70] Boqiang Zhang, Kehan Li, Zesen Cheng, Zhiqiang Hu, Yuqian Yuan, Guanzheng Chen, Sicong Leng, Yuming Jiang, Hang Zhang, Xin Li, et al. Videollama 3: Frontier multimodal foundation models for image and video understanding. *arXiv preprint arXiv:2501.13106*, 2025. 6
- [71] Hang Zhang, Xin Li, and Lidong Bing. Videollama: An instruction-tuned audio-visual language model for video understanding. *arXiv preprint arXiv:2306.02858*, 2023. 1
- [72] Kaichen Zhang, Bo Li, Peiyuan Zhang, Fanyi Pu, Joshua Adrian Cahyono, Kairui Hu, Shuai Liu, Yuanhan Zhang, Jingkan Yang, Chunyuan Li, et al. Lmms-eval: Reality check on the evaluation of large multimodal models. *arXiv preprint arXiv:2407.12772*, 2024. 1
- [73] Shilong Zhang, Peize Sun, Shoufa Chen, Min Xiao, Wenqi Shao, Wenwei Zhang, Yu Liu, Kai Chen, and Ping Luo. Gpt4roi: Instruction tuning large language model on region-of-interest. *arXiv preprint arXiv:2307.03601*, 2023. 2, 6
- [74] Yuanhan Zhang, Jinming Wu, Wei Li, Bo Li, Zeyun Ma, Ziwei Liu, and Chunyuan Li. Video instruction tuning with synthetic data. *arXiv preprint arXiv:2410.02713*, 2024. 2, 1
- [75] Bolei Zhou, Hang Zhao, Xavier Puig, Sanja Fidler, Adela Barriuso, and Antonio Torralba. Scene parsing through ade20k dataset. In *Proceedings of the IEEE Conference on Computer Vision and Pattern Recognition (CVPR)*, pages 633–641, 2017. 1
- [76] Deyao Zhu, Jun Chen, Xiaoqian Shen, Xiang Li, and Mohamed Elhoseiny. Minigt-4: Enhancing vision-language understanding with advanced large language models. *arXiv preprint arXiv:2304.10592*, 2023. 2

Object-centric Video Question Answering with Visual Grounding and Referring

Supplementary Material

6. More Implementation Details

Training Data Composition. The complete list of used datasets in training is presented in Tab. 9. For the datasets with overlapping, we select the disjoint samples during training, such as ViP-LLaVA-Instruct and LLaVA-150k.

Task	Datasets	# Samples
<i>Image Segmentation</i>		
Semantic Seg.	ADE20k [75]	20.2k
	COCO-Stuff [6]	118.3k
	Pascal-Part [10]	4.3k
	PACO-LVIS [48]	4.6k
	RefCOCO+ [21]	17k
Referring Seg.	RefCOCO [21]	22k
	RefCOCOg [40]	17k
	RefCLEF [21]	18k
Reasoning Seg.	ReasonSeg [26]	0.2k
<i>Video Segmentation</i>		
VOS	YoutubeVOS [51]	3.5k
	Ref-Youtube-VOS [51]	3.5k
Referring VOS	MeViS [15]	1.6k
	Ref-DAVIS [22]	5.3k
Reasoning VOS	ReVOS [60]	0.6k
<i>Image QA</i>		
VQA	LLaVA-150k [36]	150k
	Osprey-Conv [68]	30k
Referring VQA	Osprey-Desc [68]	60k
	ViP-LLaVA-Instruct [7]	216k
<i>Video QA</i>		
VideoQA	LLaVA-Video-OE [74]	960k
	LLaVA-Video-MC [74]	196k
	NeXT-QA-OE [59]	17k
	NeXT-QA-MC [59]	17k
	ActivityNetQA [66]	24k
	PerceptionTest [44]	2.4k
Referring VideoQA	VideoInfer (Ours)	20k

Table 9. The detailed list of training datasets. For some datasets, we only use a subset of them, such as LLaVA-Video, Osprey, and ViP-LLaVA. The sampling rate is listed in the training script.

Training Details. We utilize the dynamic resolution for Qwen2.5-VL [3] models, the max pixels of videos are set as $320 \times 28 \times 28$ for 8 frames, and the max pixels of a single image are set as $1280 \times 28 \times 28$. Images exceeding the above max pixels will be resized while maintaining their aspect ratio to fit.

Evaluation Protocols. The results of MeViS *val* and Ref-Youtube-VOS are evaluated through the online server. On VideoRefer-Bench^Q, our method processes 16 input frames. For VideoInfer, we utilize GPT-4o-2024-11-20 to evaluate

Accuracy (Acc.) and Score, following the same prompt strategy as Video-ChatGPT [39]. To evaluate region-feature based models, we convert the visual prompt (RGBA image) into the mask according to the alpha channel and then input the mask with visual input and question into these models to generate the response.

7. More Experimental Results

7.1. Quantitative Results

Method	Perception Test [44]	MVBench [30]	NEXT-QA [59]
<i>Generalist Models</i>			
LLaVA-OV-7B [28]	-	56.7	79.4
VideoLLaMA2.1-7B [13]	54.9	57.3	75.6
LLaVA-Video-7B [74]	67.9	58.6	83.2
<i>Specialist Models</i>			
Artemis [47]	47.1	34.1	-
VideoRefer-7B [69]	56.3	59.6	-
RGA3-7B (Ours)	68.7	63.8	75.3

Table 10. Comparison on general video question-answering tasks.

Results on General VideoQA Benchmarks. In addition to the referring video question-answering benchmarks, we also evaluate our architecture on general VideoQA QA tasks without visual prompts as inputs, through the LMMs-Eval toolkit [72]. As shown in Tab. 10, our model is comparable to popular general VideoQA models while possessing the ability to perform interactive referring and grounding in object-centric scenarios.

Method	val		test					
	overall		short query		long query		overall	
	gIoU	cIoU	gIoU	cIoU	gIoU	cIoU	gIoU	cIoU
LISA-7B [26]	52.9	54.0	40.6	40.6	49.4	51.0	47.3	48.4
LISA-13B [26]	56.2	62.9	44.3	42.0	54.0	54.3	51.7	51.1
VISA-7B [60]	52.7	57.8	-	-	-	-	-	-
VideoLISA-3.8B [4]	61.4	67.1	43.8	42.7	56.9	57.7	53.8	54.4
LISA++-7B [63]	64.2	68.1	49.6	51.1	59.3	61.7	57.0	59.5
RAG3-3B (Ours)	65.4	68.5	58.5	54.2	62.3	65.8	61.4	63.3
RAG3-7B (Ours)	68.7	70.2	58.7	54.1	68.5	72.1	66.1	68.3

Table 11. Comparison on validation and test set of ReasonSeg [26] for image-level reasoning object segmentation.

Results on Image Segmentation Benchmarks For image segmentation evaluation, we utilize gIoU (average per-image IoUs) and cIoU (cumulative intersection over union) on reasoning-based benchmark ReasonSeg [26] and cIoU for referring-based benchmark refCOCO(+g) [21, 40]. As shown in Tab. 11, RGA3-7B outperforms the state-of-the-art method LISA++-7B [63] on the ReasonSeg benchmark

Method	refCOCO [21]			refCOCO+ [21]			refCOCOg [40]	
	val	testA	testB	val	testA	testB	val(U)	test(U)
LISA-7B [26]	74.1	76.5	71.1	62.4	67.4	56.5	66.4	68.5
VISA-7B [60]	72.4	75.5	68.1	59.8	64.8	53.1	65.5	66.4
VideoLISA-3.8B [4]	73.8	76.6	68.8	63.4	68.8	56.2	68.3	68.8
RGA3-3B (Ours)	78.9	81.1	75.0	71.3	77.1	63.5	74.7	75.0
RGA3-7B (Ours)	79.7	82.6	76.0	73.5	78.6	67.0	76.2	75.9

Table 12. Comparison on image-level referring object segmentation datasets.

by a large margin. Moreover, on general image semantic segmentation benchmarks, such as refCOCO, RGA3-7B still outperforms recent MLLM-based methods, which indicates the strong general grounding ability of RGA3.

Robustness in Extremely Long Videos. Our work primarily addresses object-centric video tasks, which typically involve short video durations (*e.g.*, VideoRefer-Bench^Q comprises a few-second clips sourced from DAVIS or MeVIS). Although our VideoInfer incorporates longer clips (sub-minute duration) from LVOS and TAO, we acknowledge the necessity for robustness in ultra-long video. Due to the lack of appropriate benchmarks, we evaluated RGA3 on the validation set of the LongVideoBench with different duration groups:

Duration	(8s, 15s]	(15s, 60s]	(180s, 600s]	(900s, 3600s]
Accuracy	72.5	70.9	57.3	46.3

Table 13. Performance on the validation set of LongVideoBench.

More Ablations. The improvement over the previous state-of-the-art methods on video referring segmentation and question-answering is mainly from the base MLLM, the proposed STOM module, and the dataset composition in training. Additionally, we find that under the current training strategy, the performance of the individual task will decrease compared to training separately in most cases. We think this should be further addressed through multi-stage training or more diverse prompting.

Model	Training Data	MLLM	Size	Modules	VideoRefer	ReasonVOS
					Acc.	$\mathcal{J}\&\mathcal{F}$
VideoRefer	QA	SigLIP-Qwen2	7B	-	71.9	-
VideoLISA	Seg	Phi-3-V	3.8B	SAM	-	45.1
	Seg		3B	SAM	-	47.9
	Seg		3B	SAM2	-	48.7
Ours	Seg+QA	QwenVL-2.5	3B	SAM2	62.3	51.7
	Seg+QA		3B	SAM2+STOM	66.6	51.7
	Seg+QA		7B	SAM2+STOM	74.0	53.6

Table 14. Additional ablations on the design choices.

7.2. Failure Case and Future Work

In practice, due to computational limitations, we restrict RGA3’s input to 16 frames per video (Other existing object-centric VideoLLMs also suffer from this limitation). How-



Q: What’s the emotion of him?

GT: After hearing the reports, he took off his sunglasses and stared at the other person, from which we could infer that man is surprised and angry.

Pred: The man might feel angry because he is being held captive or is in a situation where he is being threatened or humiliated.

Figure 6. Failure case on VideoInfer dataset. The frames with grey masks are not selected as input to RGA3. The green box frames the video content which the man on the left reports something to the man on the right. ‘GT’ is the ground truth, and ‘Pred’ is the prediction of RGA3.

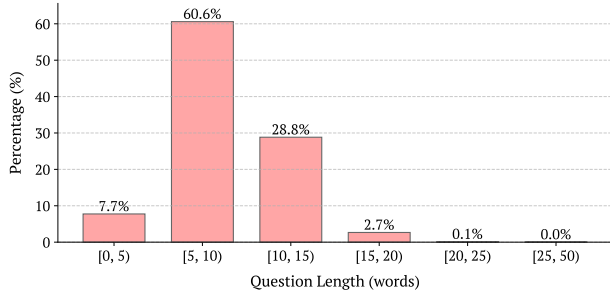
ever, in very long videos, this frame selection introduces large temporal gaps, potentially omitting critical contextual information. Our VideoInfer dataset introduces videos that contain over 1,000 frames, yet the existing models can not process the whole sequence due to computational limitations. For instance, as shown in Fig. 6, the raw video contains over 1,000 frames, yet only 16 frames are used as input. With such sparse frame sampling, the model struggles to capture a coherent sequence of events.

In this specific case, the moment when the left person reports to the right person is skipped, leading to an incorrect prediction. This issue cannot be naively addressed by extracting just one or a few visual tokens per frame, as object-level information must be preserved across frames to enable accurate object-centric reasoning. Therefore, handling long-form object-centric video reasoning remains a challenging open problem, particularly in transforming spatial and temporal detailed object-centric information into a reasonable number of tokens. We plan to explore solutions further to enhance object-centric reasoning in long videos in our future work.

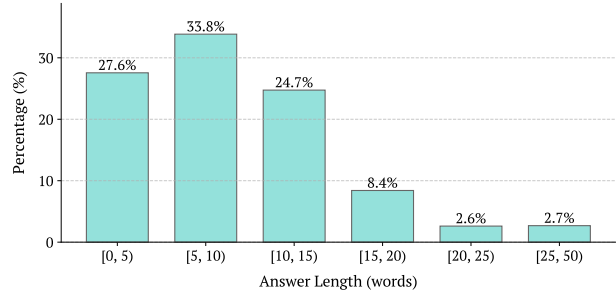
8. Discussion and Visualizations

8.1. Potential Information Loss

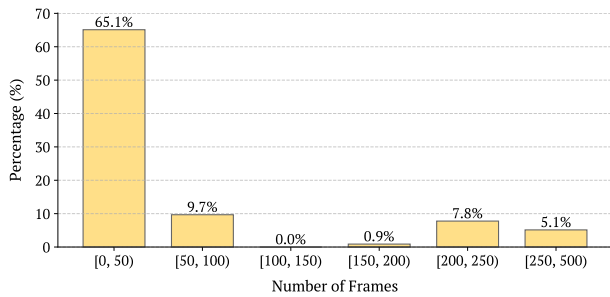
The STOM module blends prompts onto original frames with **transparency** through alpha blending, so that the objects will not be completely occluded, and the features can be reserved.



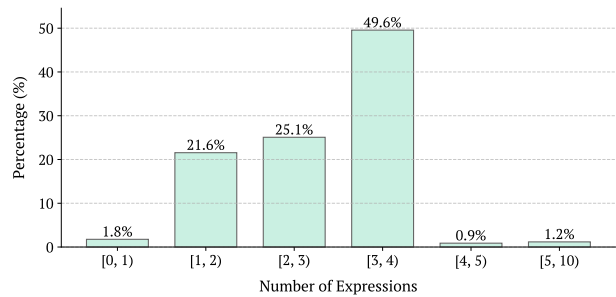
(a) Histogram of question word counts.



(b) Histogram of answer word counts.



(c) Histogram of frames per video counts.



(d) Histogram of objects per video counts.

Figure 7. Visualization of statistics of the test split of VideoInfer.

8.2. Visualization of VideoInfer Benchmark

As shown in Fig. 7, we visualize the statistics of the test split in VideoInfer. The questions range from 3 to 50 words in length, with an average of 8.4 words. Answers vary between 1 and 75 words, averaging 8.7 words. The number of frames per sample spans from 7 to over 2000, with a mean of 189.5 frames. For objects, the count ranges from 1 to 8, averaging 2.3 objects of interest per video.